Supplementary Material for "A model of aerosol evaporation kinetics in a thermodenuder" by C. D. Cappa[1]

[1] Dept. of Civil and Environmental Engineering, University of California, Davis, California

Correspondence to: C. D. Cappa (cdcappa@ucdavis.edu)

Influence of the number of bins

The TD model described in the main text requires the user to specify some number of bins, *n*, that defines the number of concentric cylinders that the system is divided into. A choice of n = 10 provides a reasonable tradeoff between overall accuracy and computational speed. Only very small changes are found in the calculated mass fraction remaining (MFR) values for $n > 10$. However, when smaller values of *n* are used the calculated MFR is greater at a given temperature, indicating less overall evaporation occurred. Results are shown in Figure S1 for calculations performed using C_{sat} = 1 μg/m^3, C_{OA} = 10 μg/m^3, ΔH_{vap} = 120 kJ/mol, d_p = 200 nm, D_i = 3 x 10^{-6} m^2/s, t_{res} = 15 seconds and the adsorbent denuder boundary condition (Case 1 in the main text). Only very small differences in the calculated MFR_{bp} are found for $n \geq 10$.

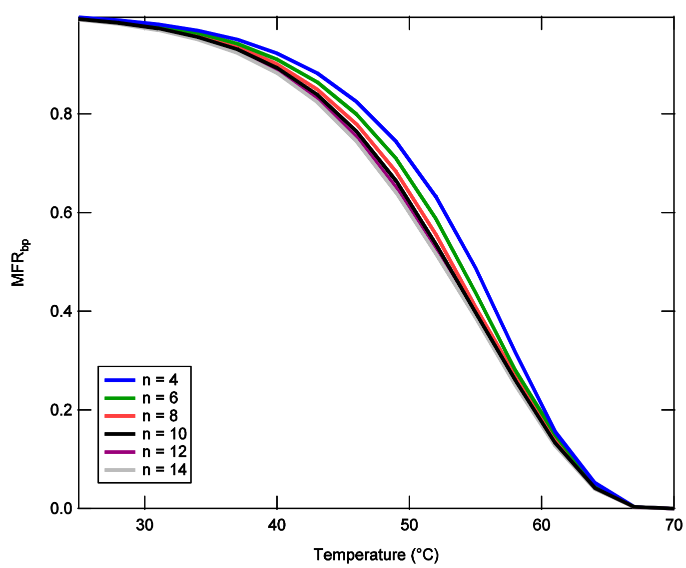

Figure S1: The calculated MFR_{bp} for different numbers of bins, *n*.

Description of Data from Figures

To facilitate comparison with other models and data sets the data from Figures 2-11 has been provided as individual text files. The specific data provided in each file for each figure is described in the tables below.

Figure 2 ("Figure 2 Data.txt")

The observations were taken from Faulhaber et al. (2009). The calculations were performed using the parameters given in Table S1. The data from the figure are included as a separate tab delimited file.

	Butanedioic Acid			Hexanedioic Acid			Decandioic Acid		
	Cappa	C&Z	Average	Cappa	C&Z	Average	Cappa	C&Z	Average
C_{sat} (μg/m^3)	1.5	6.5	3.1	0.14	1.78	0.5	0.0012	0.12	0.012
ΔH_{vap} (kJ/mol)	128	119.5	124	145.4	146	146	180	146.5	163

Table S-1. Thermodynamic parameters for the three dicarboxylic acids used to perform the calculations in Figure 2. "Cappa" = Cappa et al. (2007); C&Z = Chattopadhyay and Ziemann (2005).

Name	Description
T_But_Exp	T_d (°C) for butanedioic acid from Faulhaber et al. (2009)
MFR_But_Exp	MFR for butanedioic acid from Faulhaber et al. (2009)
T_Hex_Exp	T_d (°C) for hexanedioic acid from Faulhaber et al. (2009)
MFR_Hex_Exp	MFR for hexanedioic acid from Faulhaber et al. (2009)
T_Dec_Exp	T_d (°C) for decanedioic acid from Faulhaber et al. (2009)
MFR_Dec_Exp	MFR for decanedioic acid from Faulhaber et al. (2009)
Td	Model T_d (°C)
MFR_But_Cappa	Model MFR_{bp} for butanedioic acid using Cappa et al. thermo
MFR_But_Chat	Model MFR_{bp} for butanedioic acid using C&Z thermo
MFR_But_Mean	Model MFR_{bp} for butanedioic acid using Cappa and C&Z mean thermo
MFR_Hex_Cappa	Model MFR_{bp} for hexanedioic acid using Cappa et al. thermo
MFR_Hex_Chat	Model MFR_{bp} for hexanedioic acid using C&Z thermo
MFR_Hex_mean	Model MFR_{bp} for hexanedioic acid using Cappa and C&Z mean thermo
MFR_Dec_Cappa	Model MFR_{bp} for decanedioic acid using Cappa et al. thermo
MFR_Dec_Chat	Model MFR_{bp} for decanedioic acid using C&Z thermo
MFR_Dec_mean	Model MFR_{bp} for decanedioic acid using Cappa and C&Z mean thermo

Figure 3 (“Figure 3 Data.txt”)

Name	Description
Td	Model T_d (°C)
MFR_Profile	MFR_{bp} using velocity profile
MFR_constant	MFR_{bp} using constant velocity

Figure 4 (“Figure 4 Data.txt”)

Name	Description
Csat	Saturation concentration, C_{sat} (μg/m^3)
Dp	Particle diameter, d_p (nm)
MFR_dp_low_loading	MFR_{bp} as function of d_p at C_{OA} = 5 μg/m^3
ResidenceTime	t_{res} (s)
MFR_Csat	MFR_{bp} as function of C_{sat}
MFR_dp_high_loading	MFR_{bp} as function of d_p at C_{OA} = 150 μg/m^3
MFR_Time	MFR_{bp} as function of t_{res}

Figure 5 (“Figure 5 Data.txt)

Name	Description
Td	Model T_d (°C)
MFR_10_Absorbent	MFR_d at C_{OA} = 10 μg/m^3 for Case 1 (adsorbent denuder boundary condition)
MFR_10_NoLoss	MFR_d at C_{OA} = 10 μg/m^3 for Case 3 (no loss boundary condition)
MFR_10_Eqm	MFR_d at C_{OA} = 10 μg/m^3 for Case 2 (local equilibrium boundary condition)
MFR_100_Absorbent	MFR_d at C_{OA} = 100 μg/m^3 for Case 1 (adsorbent denuder boundary condition)
MFR_100_NoLoss	MFR_d at C_{OA} = 100 μg/m^3 for Case 3 (no loss boundary condition)
MFR_100_Eqm	MFR_d at C_{OA} = 100 μg/m^3 for Case 2 (local equilibrium boundary condition)
MFR_500_Absorbent	MFR_d at C_{OA} = 500 μg/m^3 for Case 1 (absorbent denuder boundary condition)
MFR_500_NoLoss	MFR_d at C_{OA} = 500 μg/m^3 for Case 3 (no loss boundary condition)
MFR_500_Eqm	MFR_d at C_{OA} = 500 μg/m^3 for Case 2 (local equilibrium boundary condition)

Figure 6 (“Figure 6x Data.txt”)

The data in each file (e.g. “Figure 6x Data.txt”) comes from the corresponding panel x (e.g. x = a, b, c, etc.). “Distance” is the distance from the thermodenuder entrance (in cm). The other columns “Radius_X_Y” (where X indicates the loading condition, either “high” or “low,” and Y indicates boundary condition case) are in order from closest to the TD center to closest to the TD walls.

Figure 7 ("Figure 7 Data.txt")

Name	Description
Td	Model T_d (°C)
MFR_15sec_10ug	MFR_h at t_{res} = 15 seconds and C_{OA} = 10 μg/m^3
MFR_30sec_10ug	MFR_h at t_{res} = 30 seconds and C_{OA} = 10 μg/m^3
MFR_60sec_10ug	MFR_h at t_{res} = 60 seconds and C_{OA} = 10 μg/m^3
MFR_15sec_100ug	MFR_h at t_{res} = 15 seconds and C_{OA} = 100 μg/m^3
MFR_30sec_100ug	MFR_h at t_{res} = 30 seconds and C_{OA} = 100 μg/m^3
MFR_60sec_100ug	MFR_h at t_{res} = 60 seconds and C_{OA} = 100 μg/m^3
MFR_15sec_500ug	MFR_h at t_{res} = 15 seconds and C_{OA} = 500 μg/m^3
MFR_30sec_500ug	MFR_h at t_{res} = 30 seconds and C_{OA} = 500 μg/m^3
MFR_60sec_500ug	MFR_h at t_{res} = 60 seconds and C_{OA} = 500 μg/m^3

Figure 8 ("Figure 8x Data.txt"), where x corresponds to the panel a, b, c or d

Figure 8a

Name	Description
Td	Model T_d (°C)
MFR_1000	MFR_{bp} for C_{sat} = 1000 μg/m^3
MFR_100	MFR_{bp} for C_{sat} = 100 μg/m^3
MFR_10	MFR_{bp} for C_{sat} = 10 μg/m^3
MFR_1	MFR_{bp} for C_{sat} = 1 μg/m^3
MFR_01	MFR_{bp} for C_{sat} = 0.1 μg/m^3
MFR_001	MFR_{bp} for C_{sat} = 0.01 μg/m^3
MFR_0001	MFR_{bp} for C_{sat} = 0.001 μg/m^3

Figure 8b

Name	Description
Td	Model T_d (°C)
MFR_40kJ	MFR_{bp} for ΔH_{vap} = 40 kJ/mol
MFR_60kJ	MFR_{bp} for ΔH_{vap} = 60 kJ/mol
MFR_80kJ	MFR_{bp} for ΔH_{vap} = 80 kJ/mol
MFR_100kJ	MFR_{bp} for ΔH_{vap} = 100 kJ/mol
MFR_120kJ	MFR_{bp} for ΔH_{vap} = 120 kJ/mol
MFR_140kJ	MFR_{bp} for ΔH_{vap} = 140 kJ/mol
MFR_160kJ	MFR_{bp} for ΔH_{vap} = 160 kJ/mol

Figure 8c

Name	Description
Csat	Saturation concentration (μg/m^3)
T50inv_120kJ_300nm	1/T_{50} (in 1/K) for ΔH_{vap} = 120 kJ/mol and d_p = 300 nm
T50inv_150kJ_200nm	1/T_{50} (in 1/K) for ΔH_{vap} = 150 kJ/mol and d_p = 200 nm
T50inv_faulhaber	1/T_{50} (in 1/K) from Faulhaber et al. (2009)

Figure 8d

Name	Description
DH	Enthalpy of vaporization, ΔH_{vap} (kJ/mol)
T50_DH	T_{50} (°C)

Figure 9 ("Figure 9 Data.txt")

Name	Description
dp	Particle diameter, d_p (nm)
T50_5_5	T_{50} (°C) for C_{sat} = 5 μg/m^3 and C_{OA} = 5 μg/m^3
T50_50_5	T_{50} (°C) for C_{sat} = 5 μg/m^3 and C_{OA} = 50 μg/m^3
T50_150_5	T_{50} (°C) for C_{sat} = 5 μg/m^3 and C_{OA} = 150 μg/m^3
T50_250_5	T_{50} (°C) for C_{sat} = 5 μg/m^3 and C_{OA} = 250 μg/m^3
T50_5_01	T_{50} (°C) for C_{sat} = 0.1 μg/m^3 and C_{OA} = 5 μg/m^3
T50_50_01	T_{50} (°C) for C_{sat} = 0.1 μg/m^3 and C_{OA} = 50 μg/m^3
T50_150_01	T_{50} (°C) for C_{sat} = 0.1 μg/m^3 and C_{OA} = 150 μg/m^3
T50_250_01	T_{50} (°C) for C_{sat} = 0.1 μg/m^3 and C_{OA} = 250 μg/m^3

Figure 10 ("Figure 10 Data.txt")

Name	Description
Di	Diffusion coefficient, D_i (m^2/s)
T50_300_5	T_{50} for d_p = 300 nm and C_{OA} = 5 μg/m^3
T50_300_250	T_{50} for d_p = 300 nm and C_{OA} = 250 μg/m^3
T50_100_5	T_{50} for d_p = 100 nm and C_{OA} = 5 μg/m^3

Figure 11

TarrayForTD	Model T_d (°C)
MFR_f0	MFR_{bp} for a non-volatile core that is 0% of the total particle mass (panel a)
MFR_f01	MFR_{bp} for a non-volatile core that is 10% of the total particle mass (panel a)
MFR_f02	MFR_{bp} for a non-volatile core that is 20% of the total particle mass (panel a)
MFR_f03	MFR_{bp} for a non-volatile core that is 30% of the total particle mass (panel a)
MFR_f04	MFR_{bp} for a non-volatile core that is 40% of the total particle mass (panel a)
MFR_f05	MFR_{bp} for a non-volatile core that is 50% of the total particle mass (panel a)
MFRnv_f05	MFR_{bp} for a non-volatile absorptive component that is 50% of the total particle mass (panel b)
MFRnv_f04	MFR_{bp} for a non-volatile absorptive component that is 40% of the total particle mass (panel b)
MFRnv_f03	MFR_{bp} for a non-volatile absorptive component that is 30% of the total particle mass (panel b)
MFRnv_f02	MFR_{bp} for a non-volatile absorptive component that is 20% of the total particle mass (panel b)
MFRnv_f01	MFR_{bp} for a non-volatile absorptive component that is 10% of the total particle mass (panel b)

Figure 12

"Figure 12 Data-1.txt"

Name	Description
Td	Model T_d (°C)
MFRbp	MFR_{bp} for total OA
MFRh	MFR_h for total OA
MFRd	MFR_d for total OA

"Figure 12 Data-2.txt"

Name	Description
Td	Model T_d (°C)
MFRbp_compounds	MFR_{bp} for individual compounds, in order from highest C_{sat} (100 μg/m^3) to lowest C_{sat} (10^{-3} μg/m^3)

References

Cappa, C. D., Lovejoy, E. R., and Ravishankara, A. R.: Determination of Evaporation Rates and Vapor Pressures of Very Low Volatility Compounds: A Study of the C4-C10 and C12 Dicarboxylic Acids, J. Phys. Chem. A, 111, 3099-3109, 2007.

Chattopadhyay, S., and Ziemann, P. J.: Vapor pressures of substituted and unsubstituted monocarboxylic and dicarboxylic acids measured using an improved thermal desorption particle beam mass spectrometry method, Aerosol Sci. Technol., 39, 1085-1100, 2005.

Faulhaber, A. E., Thomas, B. M., Jimenez, J. L., Jayne, J. T., Worsnop, D., and Ziemann, P. J.: Characterization of a thermodenuderparticle beam mass spectrometer system for the study of organic aerosol volatility and composition, Atmos. Meas. Tech., 2, 15-31, 2009.